ELSEVIER

PII: S1359-8368(96)00043-1

Composites Part B **28B** (1997) 243–252

1359-8368/97/$17.00

A higher order theory for modeling composite laminates with induced strain actuators

Aditi Chattopadhyay and Charles E. Seeley
Department of Mechanical and Aerospace Engineering, Arizona State University, Tempe, AZ 85287-6106, USA
(Received 3 November 1995; accepted 29 August 1996)

A refined higher order laminate theory is developed to analyze smart materials, surface bonded or embedded, in composite laminates. The analysis uses a refined displacement field which accounts for transverse shear stresses through the thickness. All boundary conditions are satisfied at the free surfaces. Non-linearities are introduced through the strain dependent piezoelectric coupling coefficients and the assumed strain distribution through the thickness. The analysis is implemented using the finite element method. The procedure is computationally efficient and allows for a detailed investigation of both the local and global effects due to the presence of actuators. The finite element model is shown to agree well with published experimental results. Numerical examples are presented for composite laminates of various thicknesses and the results are compared with those obtained using classical laminate theory. The refined theory captures important higher order effects which are not modeled by the classical laminate theory, resulting in significant deviations. © 1997 Elsevier Science Ltd

(Keywords: smart structures; composites; piezoelectric actuation)

INTRODUCTION

The concept of using adaptive materials for aerospace applications has recently received widespread attention. A key issue in the implementation of these actuators is the analysis of the primary structure with embedded and/or surface bonded actuators. In most applications of bending elements using induced strain actuation via piezoelectric materials, classical beam or plate theories have been used for the analysis. A Ritz solution was developed for anisotropic plates and verified experimentally.[1] A Bernouli–Euler type strain distribution through the thickness direction of the actuators was found to be more accurate than a uniform strain distribution.[2] Chandra and Chopra[3] investigated piezoelectric actuation of a composite beam using Vlasov theory to account for the warping behavior of the beam. Lee[4] and Wang and Rogers[5] used Heaviside functions to model piezoelectric actuators. Several authors have investigated piezoelectric actuation of laminates using a finite element approach.[6,7]

All of the analyses mentioned above are based on classical laminate theory, which assumes a linear strain distribution through the thickness and zero transverse shear stresses. Therefore, the theory must be restricted to thin plate applications. The effects of transverse shearing stresses are important in composite laminates. As a result, it is necessary to use a shear deformation theory to address moderately thick and thick laminate constructions. The stress distributions in structures actuated by piezoelectric materials are also known to be quite complex.[8] Physically, the assumption of a linear strain distribution through the thickness of a substrate material, undergoing induced strain actuation from piezoelectric materials, seems oversimplified, especially for thick plates. Chandrashekhara and Agarwal[9] and Detwiler *et al.*[10] developed finite element models for laminates with piezoelectric actuation using first order shear deformation theory. Robbins and Reddy[11] used a layer-wise theory to ascertain the level of model complexity necessary to accurately represent piezoelectric actuation of beam structures. Their study pointed out differences between the classical theory and the more sophisticated, but computationally expensive, layer-wise theory. Mitchell and Reddy[12] have also used a hybrid theory to model piezoelectric actuation and sensing in composite laminates. Lin and Rogers[13] investigated piezoelectric actuation of beam structures as a boundary value problem. Tzou and Zhong[14] investigated a thick piezoelectric continuum including shear deformation.

For the analysis of arbitrarily thick composites with surface bonded or embedded actuators, it is important to have a more effective general theory for accurately evaluating the effects of normal and transverse shear stresses on actuator performance. It has long been recognized that higher order laminate theories provide an effective solution tool for accurately predicting the deformation behavior of composites laminates subjected to bending loads. However, it is difficult to provide a consistent displacement field which accurately satisfies the stress free boundary conditions at the free surfaces while maintaining continuity of strains through the thickness. To

address this issue, a general higher order theory[15] is extended to model composites with arbitrary thicknesses and surface bonded or embedded induced strain actuators. Some higher order terms of the displacement field are identified by imposing the stress free boundary conditions. The theory is expected to more effectively model the complex stress distributions, which result from induced strain actuation, with a reasonable amount of computational effort compared to classical or first order shear deformation theory.

Although piezoelectric materials are used in the current approach, the general theory can be extended to include other adaptive materials as well. The electro-mechanical coupling coefficients for piezoelectric materials are known to be dependent upon the actual strain in the actuators,[1] although many researchers assume that these coefficients are constant. In the current analysis, the strain dependent form of these coefficients is included for greater accuracy. The finite element method is used for implementation of the analysis since it leads to a discretization of the structure which quite naturally incorporates the discontinuities due to discrete embedded actuators. However, in comparison to other finite element models, additional degrees of freedom are not used for the voltage to improve computational efficiency. The higher order theory is verified using published experimental results. Numerical examples are presented for a detailed investigation of stress and strain distributions of cantilever composite laminates with varying thicknesses.

ANALYSIS

Higher order laminate theory with piezoelectric actuation

A general higher order displacement field[15] is extended to include the effects of induced strain actuation using piezoelectric materials. Assuming that there are no defects in the composite material, such as voids or delaminations, the displacement field is continuous. The in-plane displacements are assumed to vary as cubic functions of the thickness z and the transverse displacement is independent of z (*Figure 1*). The general displacement field is defined as follows.

$$U_1(x, y, z) = u_{10}(x, y) + z\left(-\frac{\partial}{\partial x}u_{30}(x, y) + u_{11}(x, y)\right) + z^2 u_{12}(x, y) + z^3 u_{13}(x, y) \quad (1)$$

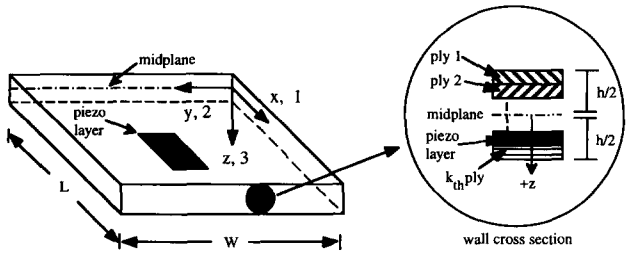

Figure 1 Composite plate orientation

$$U_2(x, y, z) = u_{20}(x, y) + z\left(-\frac{\partial}{\partial y}u_{30}(x, y) + u_{21}(x, y)\right) + z^2 u_{22}(x, y) + z^3 u_{23}(x, y)$$

$$U_3(x, y, x) = u_{30}(x, y)$$

where U_1, U_2 and U_3 are the total displacements, u_{10}, u_{20} and u_{30} denote the mid-plane displacements of a point (x, y), the partial derivatives of u_{30} represent the rotations of normals to the mid-plane corresponding to the slope of the laminate, and u_{11} and u_{21} represent the additional rotations due to shear deformation about the y and x axes, respectively. The quantities u_{12}, u_{13}, u_{22} and u_{23} represent higher order functions. This displacement field has the advantage of easily reducing to the well known classical theory if the higher order terms are eliminated. In the current work, assuming that displacements and rotations are small, a linear relationship for the kinematic equations is used.

$$\varepsilon_1 = \frac{\partial U_1}{\partial x},\ \varepsilon_2 = \frac{\partial U_2}{\partial y},\ \varepsilon_3 = 0 \quad (2)$$

$$\varepsilon_4 = \frac{\partial U_2}{\partial z} + \frac{\partial U_3}{\partial y},\ \varepsilon_5 = \frac{\partial U_1}{\partial z} + \frac{\partial U_3}{\partial x},\ \varepsilon_6 = \frac{\partial U_1}{\partial y} + \frac{\partial U_2}{\partial x}$$

where ε_{1-6} represent the linear strains. The general lamina constitutive relations are written as follows.[16]

$$\hat{\sigma} = \mathbf{Q}\hat{\varepsilon} - \mathbf{e}^{\mathrm{T}}E \text{ (converse effect)} \quad (3)$$

$$\boldsymbol{D} = \mathbf{e}\hat{\varepsilon} + \mathbf{P}E \text{ (direct effect)} \quad (4)$$

where $\hat{\sigma}$ and $\hat{\varepsilon}$ denote stress and elastic strain in the material coordinates, respectively, $\mathbf{Q}$ is the elastic stiffness matrix, $\mathbf{e}$ is the piezoelectric stress coefficient matrix, E is the electric field intensity, D is the electric displacement and $\mathbf{P}$ is the dielectric permittivity matrix. In the current analysis, only piezoelectric actuation is considered [equation (3)]. The sensor equations [equation (4)] will be developed in a future work. It can be shown that for a reasonable magnitude electric field, the piezoelectric stress coefficient matrix $\mathbf{e}$ is directly proportional to the elastic stiffness matrix $\mathbf{Q}$[4].

$$\mathbf{e} = \mathbf{dQ} \quad (5)$$

where $\mathbf{d}$ is the piezoelectric strain coefficient matrix which is defined as follows.

$$\mathbf{d} = \begin{bmatrix} 0 & 0 & d_{31} \\ 0 & 0 & d_{32} \\ 0 & 0 & d_{33} \\ 0 & d_{24} & 0 \\ d_{15} & 0 & 0 \\ 0 & 0 & d_{36} \end{bmatrix} \quad (6)$$

where it is assumed that the piezoelectric material is polarized in the thickness (3) direction as indicated in *Figure 1*. By substituting equation (5) into equation (3), the following stress–strain relationship is obtained.

$$\hat{\sigma} = \mathbf{Q}[\hat{\varepsilon} - \mathbf{d}^{\mathrm{T}}E] \quad (7)$$

where the second term in the above equation represents the induced piezoelectric strain. For the current work, within the context of plate theory, it is assumed that the electric field is

applied through the thickness direction, that is $E = [0, 0, E_3]^T$ and actuation in the thickness direction is neglected. Therefore, the induced strain (Λ) can be represented as follows.

$$\Lambda = \mathbf{d}^T E = [\Lambda_1 \ \Lambda_2 \ 0 \ 0 \ 0 \ 0]^T \tag{8}$$

where Λ is the vector of induced strain due to piezoelectric actuation, $\Lambda_1 = d_{31}E_3$ and $\Lambda_2 = d_{32}E_3$. Using this result and transforming to the laminate axes for the kth ply,[17] equation (7) simplifies to the following.

$$\begin{bmatrix} \sigma_1 \\ \sigma_2 \\ \sigma_3 \\ \sigma_4 \\ \sigma_5 \\ \sigma_6 \end{bmatrix}_k = \begin{bmatrix} \bar{Q}_{11} & \bar{Q}_{12} & 0 & 0 & 0 & \bar{Q}_{16} \\ \bar{Q}_{12} & \bar{Q}_{22} & 0 & 0 & 0 & \bar{Q}_{26} \\ 0 & 0 & 0 & 0 & 0 & 0 \\ 0 & 0 & 0 & \bar{Q}_{44} & \bar{Q}_{45} & 0 \\ 0 & 0 & 0 & \bar{Q}_{45} & \bar{Q}_{55} & 0 \\ \bar{Q}_{16} & \bar{Q}_{26} & 0 & 0 & 0 & \bar{Q}_{66} \end{bmatrix}_k \begin{bmatrix} \varepsilon_1 - \Lambda_1 \\ \varepsilon_2 - \Lambda_2 \\ \varepsilon_3 \\ \varepsilon_4 \\ \varepsilon_5 \\ \varepsilon_6 \end{bmatrix}_k \tag{9}$$

or, in vector form,

$$\sigma_k = \bar{\mathbf{Q}}[\varepsilon_k - \Lambda_k] \tag{10}$$

It is important to note that Λ_k is non-zero only in the piezoelectric layers.

From equation (9), it can be seen that the transverse shear stress terms are uncoupled and are written as follows.

$$\begin{bmatrix} \sigma_4 \\ \sigma_5 \end{bmatrix} \begin{bmatrix} \bar{Q}_{44} & \bar{Q}_{45} \\ \bar{Q}_{45} & \bar{Q}_{55} \end{bmatrix} \begin{bmatrix} \varepsilon_4 \\ \varepsilon_5 \end{bmatrix} \tag{11}$$

where σ_4 and σ_5 denote the transverse shear stresses.

It is important to note that the general displacement field proposed in equation (1) does not satisfy the boundary conditions at the top and bottom surfaces. However, it is necessary that the transverse shear stresses (σ_4 and σ_5) vanish at the free surfaces. By imposing these conditions, some higher order terms are identified as follows.

$$\sigma_4\left(x, y, \pm\frac{h}{2}\right) = 0, \ \sigma_5\left(x, y, \pm\frac{h}{2}\right) = 0 \tag{12}$$

where h is the plate thickness (*Figure 1*). For orthotropic laminates, these conditions are equivalent to the requirement that the corresponding strains be zero at these surfaces.

$$\varepsilon_4\left(x, y, \pm\frac{h}{2}\right) = 0, \ \varepsilon_5\left(x, y, \pm\frac{h}{2}\right) = 0 \tag{13}$$

where ε_4 and ε_5 denote the transverse shear strains. Equations 12 and 13 provide four equations which determine that u_{12} and $u_{22} = 0$ and allow the higher order terms u_{13} and u_{23} to be determined in terms of the lower order terms. Note that the piezoelectric strains (Λ) do not enter into the determination of the transverse shear stresses. The refined displacement field, which contains the same number of unknown functions as the first order theory while providing greater accuracy, is written as follows.

$$U_1 = u_{10} + z\left(-\frac{\partial u_{30}}{\partial x} + u_{11}\right) - \frac{4}{3}\frac{z^3}{h^2}u_{11} \tag{14}$$

$$U_2 = u_{20} + z\left(-\frac{\partial u_{30}}{\partial y} + u_{21}\right) - \frac{4}{3}\frac{z^3}{h^2}u_{21}$$

$$U_3 = u_{30}$$

The laminate force and moment resultants for the bending and extension terms ($\mathbf{N}_B$) are obtained by integrating the appropriate stresses through the thickness in the z direction.

$$\mathbf{N}_B = \mathbf{A}_B\varepsilon_B - \mathbf{A}_{B_p}\Lambda_B \tag{15}$$

where

$$\mathbf{N}_B = [N_i \ M_i \ P_i]^T \ (i = 1, 2, 6) \tag{16}$$

and the forces (N_i), moments (M_i) and higher order moments (P_i) are calculated as follows.

$$(N_i, M_i, P_i) = \int_{-h/2}^{h/2} \sigma_i \, (1, z, z^3)\mathrm{d}z \ (i = 1, 2, 6) \tag{17}$$

The laminate stiffness matrix for the bending terms is formulated as follows.

$$\mathbf{A}_B = \begin{bmatrix} [A_{ij}] & [B_{ij}] & [E_{ij}] \\ & [D_{ij}] & [F_{ij}] \\ sym & & [H_{ij}] \end{bmatrix} \ (i, j = 1, 2, 6) \tag{18}$$

where

$$(A_{ij}, B_{ij}, D_{ij}, E_{ij}, F_{ij}, H_{ij})$$

$$= \int_{-h/2}^{h/2} \bar{Q}_{ij} \, (1, z, z^2, z^3, z^4, z^6)\mathrm{d}z \ (i, j = 1, 2, 6) \tag{19}$$

The matrix $\mathbf{A}_{B_p}$ in equation (15) is similar to $\mathbf{A}_B$, but includes the effects due to piezoelectric actuation (Λ_B) and depends on the manner in which the electric field is applied. It will be discussed in more detail shortly. The bending and extension strains are represented by their respective mid-plane strains and curvatures as follows.

$$\varepsilon_B = [\varepsilon_i^0 \ \kappa_i^0 \ \kappa_i^2]^T \ (i = 1, 2, 6) \tag{20}$$

where

$$\varepsilon_1 = \varepsilon_1^0 + z\kappa_1^0 + z^3\kappa_1^2 \tag{21}$$

$$\varepsilon_2 = \varepsilon_2^0 + z\kappa_2^0 + z^3\kappa_2^2 \tag{22}$$

$$\varepsilon_6 = \varepsilon_6^0 + z\kappa_6^0 + z^3\kappa_6^2 \tag{23}$$

and

$$\varepsilon_1^0 = \frac{\partial u_{10}}{\partial x}, \ \kappa_1^0 = \frac{\partial u_{11}}{\partial x} - \frac{\partial^2 u_{30}}{\partial x^2}, \ \kappa_1^2 = -\frac{4}{3h^2}\frac{\partial u_{11}}{\partial x} \tag{24}$$

$$\varepsilon_2^0 = \frac{\partial u_{20}}{\partial y}, \ \kappa_2^0 = \frac{\partial u_{21}}{\partial y} - \frac{\partial^2 u_{30}}{\partial y^2}, \ \kappa_2^2 = -\frac{4}{3h^2}\frac{\partial u_{21}}{\partial y}$$

$$\varepsilon_6^0 = \frac{\partial u_{10}}{\partial y} + \frac{\partial u_{20}}{\partial x}, \ \kappa_6^0 = \frac{\partial u_{11}}{\partial y} + \frac{\partial u_{21}}{\partial x} - 2\frac{\partial^2 u_{30}}{\partial x \partial y},$$

$$\kappa_6^2 = \frac{4}{3h^2}\left(\frac{\partial u_{11}}{\partial y} + \frac{\partial u_{21}}{\partial x}\right)$$

The transverse shear force resultant terms ($\mathbf{N}_T$) are derived as follows.

$$\mathbf{N}_T = \mathbf{A}_T \varepsilon_T \tag{25}$$

where

$$\mathbf{N}_T = [Q_i \; R_i]^T \; (i = 4, 5) \tag{26}$$

and the transverse shear forces (Q_i and R_i) are calculated as follows.

$$(Q_2, R_2) = \int_{-h/2}^{h/2} \sigma_4 (1, z^2) dz \tag{27}$$

$$(Q_1, R_1) = \int_{-h/2}^{h/2} \sigma_5 (1, z^2) dz \tag{28}$$

The laminate stiffness matrix for the transverse shear terms is formulated as follows.

$$\mathbf{A}_T = \begin{bmatrix} [A_{ij}] & [D_{ij}] \\ sym & [F_{ij}] \end{bmatrix} \; (i, j = 4, 5) \tag{29}$$

where

$$(A_{ij}, D_{ij}, F_{ij}) = \int_{-h/2}^{h/2} \bar{Q} (1, z^2, z^4) dz \; (i = 4, 5) \tag{30}$$

The transverse strains are also represented by their respective mid-plane strains and curvatures.

$$\varepsilon_T = [\varepsilon_i^0 \; \kappa_i^2]^T \; (i = 4, 5) \tag{31}$$

where

$$\varepsilon_4 = \varepsilon_4^0 + z^2 \kappa_4^2 \tag{32}$$

$$\varepsilon_5 = \varepsilon_5^0 + z^2 \kappa_5^2 \tag{33}$$

and

$$\varepsilon_4^0 = u_{21}, \; \varepsilon_5^0 = u_{11}, \; \kappa_4^2 = -\frac{4}{h^2} u_{21}, \; \kappa_5^2 = -\frac{4}{h^2} u_{11} \tag{34}$$

All of the above transverse shear terms are important in the analysis of the composite, but are assumed to be zero in the classical laminate theory.

Forces due to piezoelectric actuation

The forces and moments produced as a result of piezoelectric actuation are now discussed. It is assumed that the piezoelectric actuators are either surface bonded or are embedded in the composite laminate such that the piezoelectric material replaces the substrate material in the corresponding plies which contain actuators. The electromechanical coupling between the applied electric field and the induced strain in the piezoelectric material is governed by the d_{31} and d_{32} coupling coefficients, which are piezoelectric material properties and are defined as follows.

$$\begin{bmatrix} \Lambda_1 \\ \Lambda_2 \end{bmatrix} = \begin{bmatrix} d_{31} \\ d_{32} \end{bmatrix} E_3 \tag{35}$$

where E_3 is the applied electric field through the thickness of the actuator. Constant values of d_{31} and d_{32} have been assumed by many researchers.[2–15] However, as shown by Crawley and Lazarus,[1] these coefficients depend on the actual strain in the actuator as well. Functional relationships for these coupling coefficients are obtained by fitting a quadratic polynomial through the strain *versus* electric field data for an unconstrained piezoelectric actuator shown in *Figure 2*. Here, the non-linearity is due primarily to the actual strain in the actuator as the electric field is increased. The induced strain is equal to the actual strain in an unconstrained actuator and is represented in each orthogonal direction as follows.

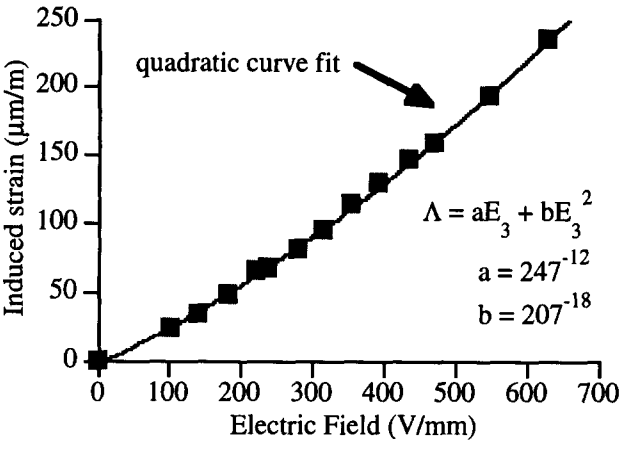

Figure 2 Experimental relationship between applied electric field and induced strain

$$\Lambda = \varepsilon = aE_3 + bE_3^2 \tag{36}$$

where a and b are constants determined from a least squares curve fit. Solving for the strain dependent coupling coefficient, the following expression is obtained.

$$d(\varepsilon) = \frac{A}{2} + \frac{A}{2}\sqrt{1 + \frac{4B\varepsilon}{A^2}} \tag{37}$$

where $d(\varepsilon)$ is the strain dependent coupling coefficient. Expanding the term under the radical using a binomial expansion and substituting the resulting expression into equation (35) yields the following relationship.

$$\begin{bmatrix} \Lambda_1 \\ \Lambda_2 \end{bmatrix} = \begin{bmatrix} d_{31} \\ d_{32} \end{bmatrix} E_3 = \left[\begin{Bmatrix} a \\ a \end{Bmatrix} + \frac{b}{a} \begin{Bmatrix} |\varepsilon_1| \\ |\varepsilon_2| \end{Bmatrix} \right] E_3 \tag{38}$$

where Λ_1 and Λ_2 are the induced strains, E_3 is the applied electric field, ε_1 and ε_2 are the actual strains, and a and b are experimentally determined constants. In the current research, it is assumed that the above expression is independent of the signs of the actual strains. Therefore, the absolute values of the actual strains (ε_1 and ε_2) are used. Otherwise, it is possible that the coefficients d_{31} and d_{32} could approach zero values for large negative strains. In such a situation, an infinitely large applied electric field would produce no induced strain, which is not practical. This issue was not addressed in ref. [1]. It is important to note that the first term on the right hand side of equation (38) is constant, while the second term is the strain dependent component.

The dependence of the induced strain on the actual strain significantly complicates the analysis of composite laminates. An iterative approach is to start with guessed values of d_{31} and d_{32}. Next, the displacements and strains are calculated and the initial guesses are checked using equation

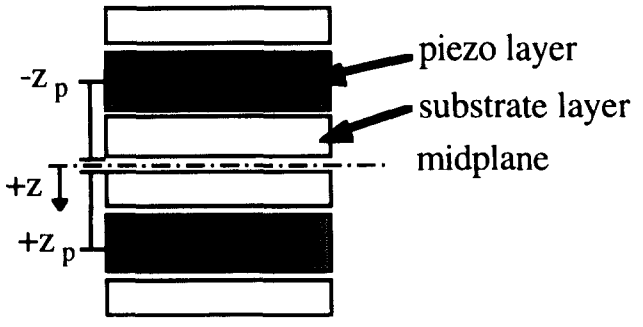

Figure 3 Symmetric piezoelectric layer placement in composite laminate

(38). The process must be repeated several times until close agreement is obtained. This approach is quite inefficient and computationally expensive. A more robust procedure is used here, which is based on the assumption that the strain distribution is assumed *a priori* based on the actuation mode. Consider the case where two actuators are placed in a symmetric configuration, with respect to the neutral axis, and are actuated with equal, but opposite, electric fields to produce bending in the composite substrate (*Figure 3*). The mid-plane strains are small in this case and can be neglected for the determination of d_{31} and d_{32}. Therefore, the actual strains used in this relationship depend only on the curvatures. Assuming that positive bending is induced, the forces and moments due to piezoelectric actuation from equation (15) are determined as follows.

$$\mathbf{A}_{\mathrm{B_p}}\Lambda_{\mathrm{B}} = \mathbf{A}_{\mathrm{a}}'\Lambda_{\mathrm{a}} + \mathbf{A}_{\mathrm{b}}'\Lambda_{\mathrm{b}} \tag{39}$$

where

$$\mathbf{A}_{\mathrm{a}}' = \begin{bmatrix} [0] & [B_{ij}'] & [E_{ij}'] \\ [B_{ij}'] & [0] & [0] \\ [E_{ij}'] & [0] & [0] \end{bmatrix} \quad (i, j = 1, 2, 6) \tag{40}$$

$$\mathbf{A}_{\mathrm{b}}' = \begin{bmatrix} [0] & [0] & [0] \\ [0] & [D_{ij}'] & [F_{ij}'] \\ [0] & [F_{ij}'] & [H_{ij}'] \end{bmatrix} \quad (i, j = 1, 2, 6) \tag{41}$$

and the elements of $\mathbf{A}_{\mathrm{a}}'$ and $\mathbf{A}_{\mathrm{b}}'$ are defined as follows.

$$(B_{ij}', E_{ij}') = a(-E_3)\int_{+z_p} \bar{Q}_{ji}(z, z^3)\mathrm{d}z + a(E_3)\int_{-z_p} \bar{Q}_{ji}(z, z^3)\mathrm{d}z \ (i, j = 1, 2, 6) \tag{42}$$

$$(D_{ij}', F_{ij}', H_{ij}') = -\frac{b}{a}(-E_3)\int_{+z_p} \bar{Q}_{ji}(z^2, z^4, z^6)\mathrm{d}z + \frac{b}{a}(E_3)\int_{-z_p} \bar{Q}_{ji}(z^2, z^4, z^6)\mathrm{d}z \ (i, j = 1, 2, 6) \tag{43}$$

where z_{p} indicates integration through a piezoelectric layer only (*Figure 3*). The appearance of the first negative sign in equation (43) is the result of the assumed strain distribution for positive induced bending and the determination of absolute values for ε_1 and ε_2. The vectors Λ_{a} and Λ_{b} are non-zero only in the piezoelectric layers and are defined as follows.

$$\Lambda_a = [1\ 1\ 0\ 0\ 0\ 0\ 0\ 0]^{\mathrm{T}} \tag{44}$$

$$\Lambda_b = [0\ 0\ 0\ \kappa_1^0\ \kappa_2^0\ 0\ \kappa_1^2\ \kappa_2^2\ 0]^{\mathrm{T}}$$

The laminate forces from equation (15) are now re-written as follows.

$$\mathbf{N}_{\mathrm{B}} = \mathbf{A}_{\mathrm{B}}\varepsilon_{\mathrm{B}} - \mathbf{A}_{\mathrm{a}}'\Lambda_{\mathrm{a}} - \mathbf{A}_{\mathrm{b}}'\Lambda_{\mathrm{b}} \tag{45}$$

Classical laminate theory

The standard classical laminate theory (CLT) is used for a comparison of the developed refined higher order theory and is obtained by setting the higher order terms of equations (1) or (14) to zero. Since the transverse shear stresses are zero, the constitutive relationships for each ply reduce to the following form.

$$\begin{bmatrix} \sigma_1 \\ \sigma_2 \\ \sigma_6 \end{bmatrix}_k = \begin{bmatrix} \bar{Q}_{11} & \bar{Q}_{12} & \bar{Q}_{16} \\ \bar{Q}_{12} & \bar{Q}_{22} & \bar{Q}_{26} \\ \bar{Q}_{16} & \bar{Q}_{26} & \bar{Q}_{66} \end{bmatrix}_k \begin{bmatrix} \varepsilon_1 - \Lambda_1 \\ \varepsilon_2 - \Lambda_2 \\ \varepsilon_6 \end{bmatrix}_k \tag{46}$$

where Λ_1 and Λ_2 represent the induced piezoelectric strains as before. Although the strains are continuous from ply to ply, the elastic constants may vary and the stresses are not necessarily continuous.

Finite element modeling

The principle of virtual displacements is used to derive the finite element model and is stated in continuous form as follows.

$$\delta\Pi = \delta U_B + \delta U_T - \delta W = 0 \tag{47}$$

where δU_{B} is the internal strain energy due to bending and extension, δU_{T} is the internal strain energy due to transverse shear and δW is the work done by an applied external distributed load $p(x, y)$. Although the complete equilibrium equations and associated boundary conditions can be derived from equation (47), these equations are not presented here due to length restrictions. The linear finite element equations are obtained as follows.

$$(\mathbf{K} - \mathbf{K}_{\mathrm{p}})\mathbf{w} = \mathbf{F} + \mathbf{F}_{\mathrm{p}} \tag{48}$$

where the quantities $\mathbf{K}_{\mathrm{e}}$ and $\mathbf{F}_{\mathrm{e}}$ represent the standard stiffness matrix and force vector due to a distributed load, $\mathbf{F}_{\mathrm{P}}^{\mathrm{e}}$ is the force vector due to the constant portion of the piezoelectric actuation and $\mathbf{K}_{\mathrm{P}}^{\mathrm{e}}$ is the resultant matrix due to the strain dependent portion of the piezoelectric actuation. The above set of equations are solved only once to determine all the necessary quantities, including the strain dependent piezoelectric coefficients d_{31} and d_{32}. However, due to the necessary assumptions regarding the determination of these coefficients, all actuators must be energized in a symmetric, bimorph configuration with the same electric field resulting in positive bending which is typical of many practical applications. Further details of the finite element modeling are presented in the Appendix.

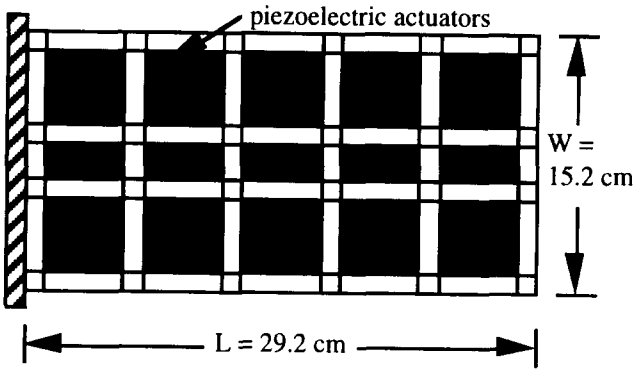

Figure 4 Cantilever plate for experimental validation

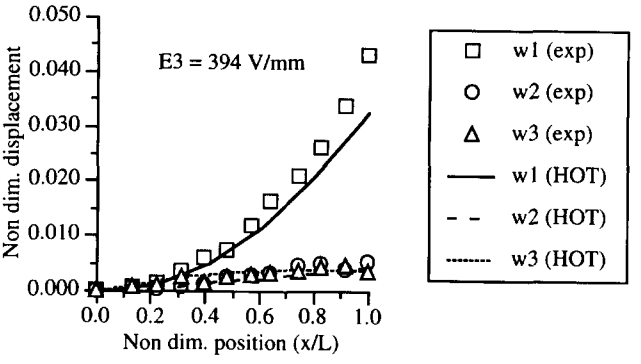

Figure 6 Non-dimensional static mode shapes for Gr/Ep $[0°/45°/-45°]_s$ plate

RESULTS

The developed refined higher order theory provides a framework for the analysis of composite laminates of arbitrary thickness with embedded actuators and is computationally efficient. Numerical results are presented first to compare the higher order theory with published experimental results to ascertain its validity. Next, strain and stress distributions resulting from piezoelectric actuation are presented for a cantilever composite plate with varying thicknesses. Differences between the developed higher order theory and the classical laminate theory are discussed.

Experimental verification

The results from the current approach are compared to experimental results obtained by Crawley and Lazarus.[1] The test case consists of a cantilever laminate as shown in *Figure 4*. Fifteen pairs of piezoceramic PZT actuators are surface bonded to either an aluminum or a graphite/epoxy plate with stacking sequences $[0°/45°/-45°]_s$ and $[30°/30°/0°]_s$. Material properties are identical to those used in ref.[18] The finite element model comprises 77 elements and a total of 616 degrees of freedom.

The thicknesses of the composite laminate and the surface bonded piezoelectric actuators are 0.83 mm and 0.25 mm, respectively. Including the actuators, the plate can be considered a "thin" plate since the ratio $L/h = 220$. The bimorph piezoelectric actuator pairs are energized with opposite electric fields to produce plate bending. Good agreement is observed between the current higher order based finite element model and the experimental results for both the aluminum and Gr/Ep plates as shown in *Figures 5–7*. The non-dimensional quantities shown include the plate bending (w_1), twist (w_2) and camber or transverse bending (w_3).[1]

Investigation of composite laminate with embedded actuators

Next, a detailed investigation of the stresses and strains throughout a composite laminate is considered. The test article is a cantilever $[0°/0°/45°/-45°]_s$ Gr/Ep laminate with embedded PZT actuators with the same material properties used in the previous section. The laminate is 25.0 cm in length and 12.5 cm in width (*Figure 8*). The outermost plies have thicknesses of 0.050 h, the adjacent plies are 0.200 h thick, and the remaining plies are 0.125 h thick, where h is the total laminate thickness indicated in *Figure 1*. The piezoelectric actuators are embedded such that they replace the outermost plies in sections of the laminate where they are located. Equal but opposite electric fields of magnitude 500 V/mm are applied through the thicknesses of each actuator pair to produce bending which results in a tip displacement in the positive z direction (*Figure 8*). All other loads are assumed to be zero (that is, $p(x, y) = 0$). The actuators are located centrally on the

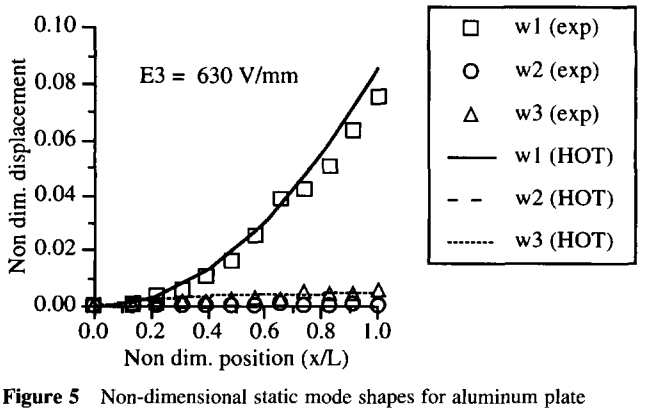

Figure 5 Non-dimensional static mode shapes for aluminum plate

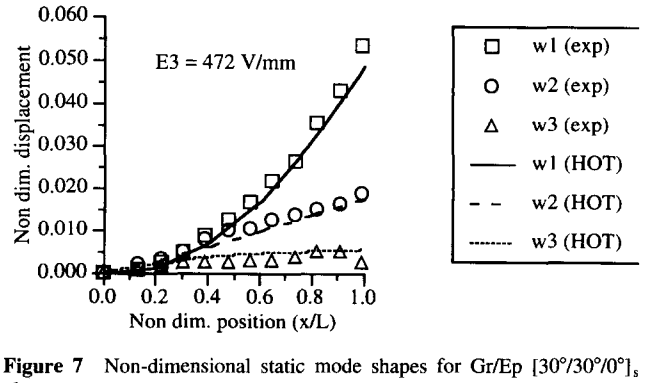

Figure 7 Non-dimensional static mode shapes for Gr/Ep $[30°/30°/0°]_s$ plate

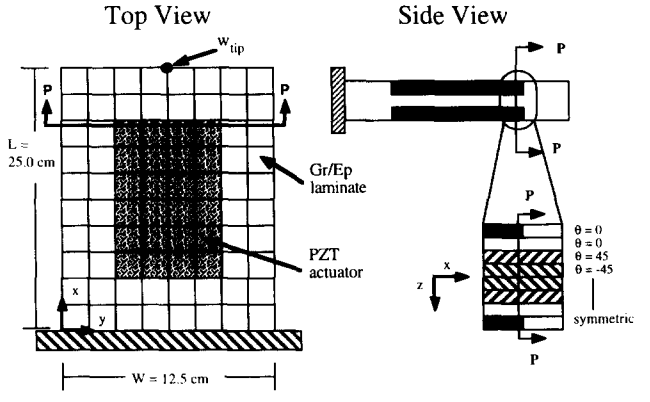

Figure 8 Cantilever Gr/Ep$[0°/0°/45°/-45°]_s$ laminate with piezoelectric actuators: top and side views

laminate and the actuator length and width are 15 cm and 6.25 cm, respectively. The values of the experimentally determined quantities (a and b) used to calculate d_{31} and d_{32} are $a = 247 \times 10^{-12}$m/V and $b = 207 \times 10^{-18}$m/V [equation (42) and *Figure 2*]. The finite element model comprises 80 equal-sized elements with 630 total degrees of freedom. For comparison, the equivalent model using the classical laminate theory consists of 450 degrees of freedom.

Strains and stresses are calculated throughout the laminate at the elemental gauss points used in the stiffness matrix assembly. In *Figures 9–12*, the axial strain and stress distributions are presented, through the thickness, close to the center of section P–P, as indicated in *Figure 8*. This section is chosen to study the effects of induced strain actuation where local stresses are expected to be large without the influence of global boundary conditions such as the fixed end. The transverse shear strain distribution (ε_{13}) is presented in *Figure 13* at this same location. Results are presented for laminates of length to thickness ratio $L/h = 10$

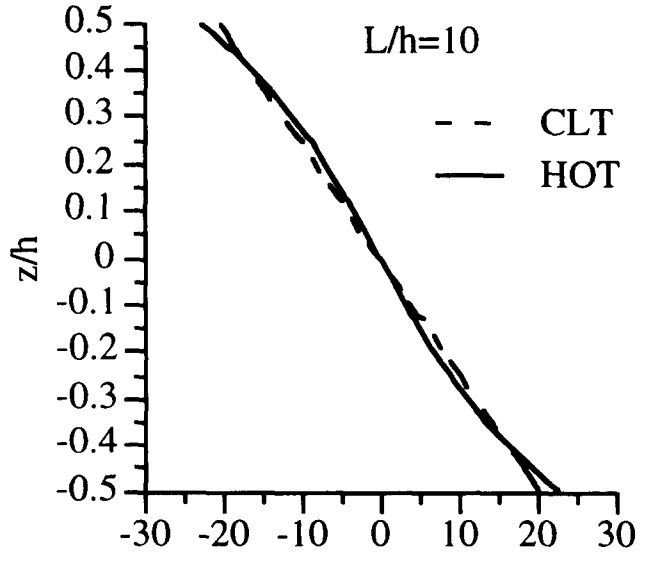

Figure 9 Axial strain ($L/h = 10$)

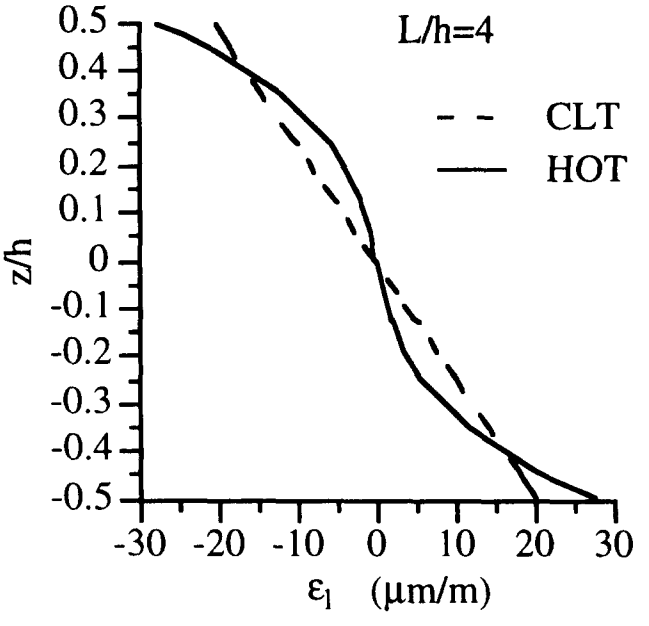

Figure 10 Axial strain ($L/h = 4$)

and 4, which are considered moderately thick and very thick, respectively, using both the classical laminate theory (CLT) and the higher order theory (HOT).

Figures 9 and *10* present the strain distribution through the thickness for the moderately thick and very thick laminates, respectively. Although the strain distribution is slightly non-linear for the moderately thick laminate (*Figure 9*), the refined theory shows that it is significantly non-linear for the very thick laminate (*Figure 10*). The CLT does not accurately capture this complexity. The strain is larger near the free edge of the laminate due to local deformation from the piezoelectric actuation in the outermost plies, but drops off more rapidly away from the actuator near the neutral axis as compared to the CLT.

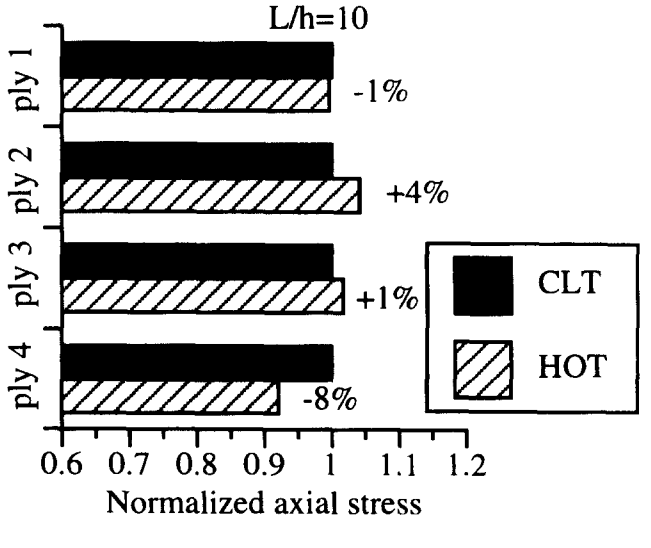

Figure 11 Normalized axial stress ($L/h = 10$)

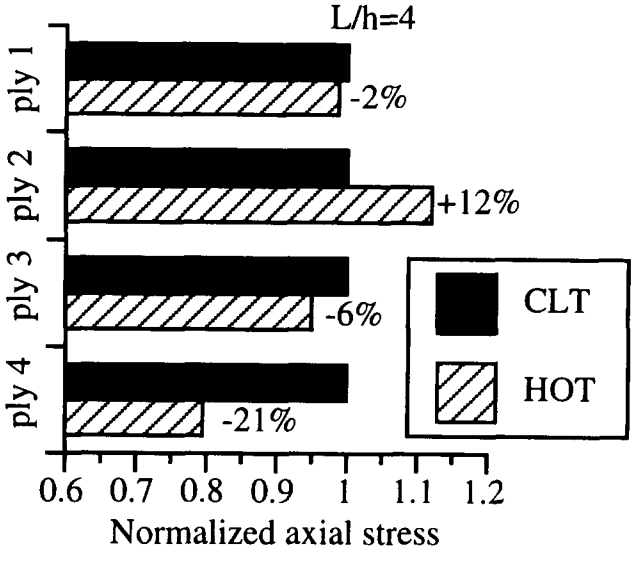

Figure 12 Normalized axial stress ($L/h = 4$)

The stresses due to the piezoelectric actuation are presented in *Figures 11* and *12* for four plies (one half of the laminate thickness). The stresses in the other half of the laminate are equal, but opposite, due to the symmetry of the laminate and the actuation mode. In these figures, the stresses are normalized, ply by ply, to the largest value predicted by CLT. The deviations in the stresses predicted by the HOT and the CLT are small in the outermost ply, which is the piezoelectric layer. This is because the effect of the additional strain predicted by the HOT is offset by larger values of the strain dependent piezoelectric coefficients, and thus the induced strain Λ [see equation (10)]. In the adjoining substrate ply, where the induced strain is zero, the stress is significantly larger than that predicted by the CLT. However, the stresses in the plies away from the actuator and near the mid-plane are less than those predicted by the

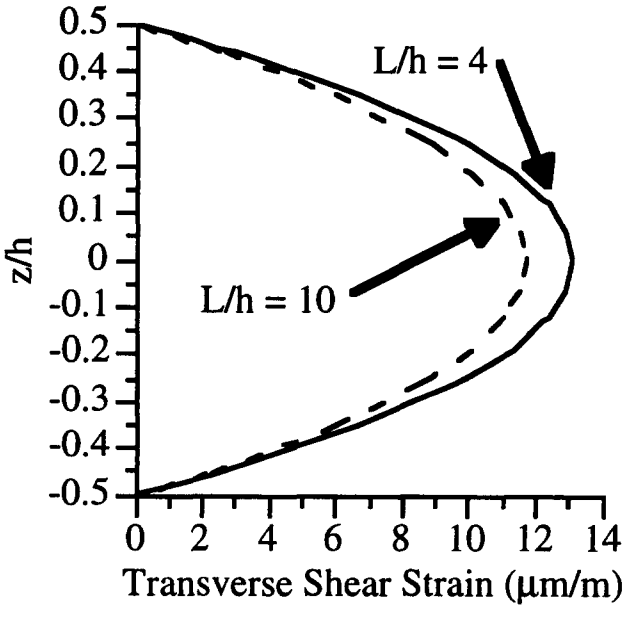

Figure 13 Transverse shear strain (ε_{13})

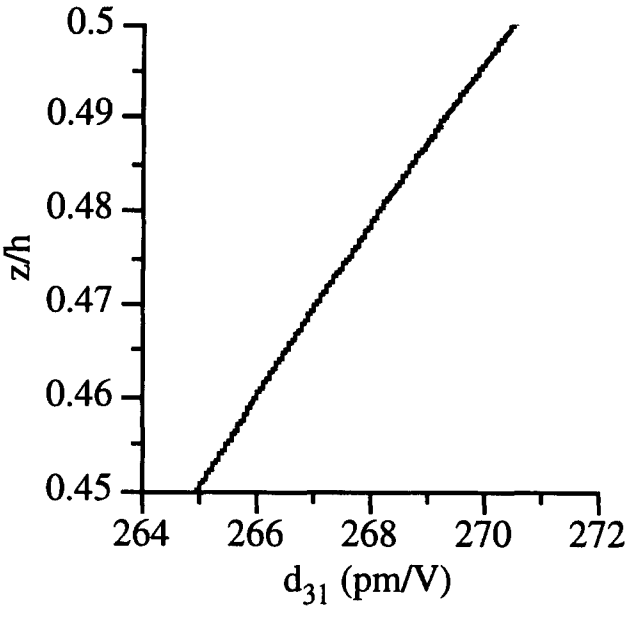

Figure 14 Variation in d_{31} through piezoelectric layer

CLT due to the local nature of the stresses resulting from piezoelectric actuation. These results indicate that the contribution of the higher order terms from the refined displacement field is significant and is important in the prediction of the strains and stresses through the thickness of composite laminates, particularly near the source of the induced strain actuation.

The distribution of the transverse shear strain (ε_{13}) through the thickness of the laminate is presented in *Figure 13* for both L/h values and shows significant variation through the thickness. The maximum value occurs at the mid-plane of the plate. As expected, the strain increases as the thickness of the plate is increased. It must be noted that the transverse strains are assumed to be zero in the classical theory.

The variation in the strain dependent piezoelectric coefficients d_{31} and d_{32} is also found to be significant. This variation is presented through the thickness of one actuator layer in *Figure 14* and is cubic in nature, although it appears to be almost linear for a single layer. Not only does the value vary through the thickness of the actuator, it is significantly different from the constant value normally used ($d_{31} = 254$ pm/V) which is determined at a state of zero strain.

CONCLUDING REMARKS

A refined higher order laminate theory was presented to investigate the actuation mechanism of piezoelectric materials embedded in composite laminates of arbitrary thickness. Some higher order terms of the displacement field were identified by imposing stress free boundary conditions. Non-linearities were introduced through both the higher order displacement field and the strain dependent piezoelectric coefficients. The finite element method was used for

implementation of the theory. The results were validated with published experimental data. Numerical results were also presented for cantilever composite laminates of varying thicknesses to investigate differences between the classical laminate theory (CLT) and the developed higher order theory (HOT). The following important observations were made from this study.

(1) The developed theory provides a computationally efficient framework for the analysis of composite laminates of arbitrary thickness with embedded or surface bonded induced strain actuators.
(2) Significant deviations are observed between the HOT and the CLT in the strain and stress distributions through the thickness, which indicates the importance of the higher order terms in the refined displacement field.
(3) The HOT efficiently captures the localized nature of the stresses near the actuators.
(4) The induced strain varies significantly as a result of the strain dependent piezoelectric coefficients. These coefficients are efficiently determined without the need for iteration.

ACKNOWLEDGEMENTS

This research was supported by NASA Langley Research Center, Grant Number NAG-1-1648, Technical monitor, Jennifer Heeg.

REFERENCES

1 Crawley, E. F. and Lazarus, K. B., Induced strain actuation of isotropic and anisotropic plates. *AIAA J.*, 1991, **29**(5), 944–951.
2 Crawley, E. F. and Anderson, E. H., Detailed models of piezoceramic actuation of beams. In *Proc. 30th AIAA/ASME/ASCE/AHS/ASC Structures, Structural Dynamics and Materials Conference*. Mobile, AL, 3–5 April, 1989, pp. 2000–2010.
3 Chandra, R. and Chopra, I., Structural modeling of composite beams with induced strain actuators. *AIAA J.*, 1993, **31**(9), 1692–1701.
4 Lee, C. K., Theory of laminated piezoelectric plates for the design of distributed sensors/actuators. Part 1: Governing equations and reciprocal relationships. *J. Acoust. Soc. Am.*, 1990, **87**(3), 1144–1158.
5 Wang, B. -T. and Rogers, C. A., Laminate plate theory for spatially distributed induced strain actuators. *J. Compos. Mater.*, 1991, **25**, 433–452.
6 Hwang, W. S., Park, H. C. and Hwang, W., Vibration control of a laminated plate with piezoelectric sensor/actuator: Finite element formulation and modal analysis. *J. Int. Mater. Syst. Struct.*, 1993, **4**, 317–329.
7 Shieh, R. C., Finite element formulation for dynamic response analysis of multiaxially active 3-D piezoelectric beam element structures. In *Proc. 34th AIAA/ASME/ASCE/AHS/ASC Structures, Structural Dynamics and Materials Conference*, LaJolla, CA, 19–22 April 1993, pp. 3250–3260.
8 Mollenhauer, D. H. and Griffen, O. H. Jr, Induced strain of actuation of surface bonded piezoceramic patches: A numerical and experimental study. *J. Int. Mater. Syst. Struct.*, 1994, **5**, 335–362.
9 Chandrashekhara, K. and Agarwal, A. N., Active vibration control of laminated composite plates using piezoelectric devices: A finite element approach. *J. Int. Mater. Syst. Struct.*, 1993, **4**, 496–508.
10 Detwiler, D. T., Shen, M. -H. H. and Venkayya, V. B., Finite element analysis of laminated composite structures containing distributed piezoelectric actuators and sensors. *Finite Elements in Analysis and Design*, 1995, **20**, 87–100.
11 Robbins, D. H. and Reddy, J. N., Analysis of piezoelectrically actuated beams using a layerwise displacement theory. *Compos. Struc.*, 1991, **41**(2), 265–279.
12 Mitchell, J. A. and Reddy, J. N., A refined hybrid plate theory for composite laminates with piezoelectric laminate. *Int. J. Solids Struct.*, 1995, **32**(16), 2345–2367.
13 Lin, M. W. and Rogers, C. A., Modeling of the actuation mechanism in a beam structure with induced strain actuators. In *Proc. 34th AIAA/ASME/ASCE/AHS/ASC Structures, Structural Dynamics and Materials Conference*, LaJolla, CA, 1993, pp. 3608–3617.
14 Tzou, H. S. and Zhong, J. P., Electromechanics and vibrations of piezoelectric shell distributed systems. *J. Dynamic Systems, Measurement & Control*, 1993, **115**, 506–517.
15 Reddy, J. N., A general non-linear third-order theory of plates with moderate thickness. *Int. J. Non-Linear Mech.*, 1990, **25**(6), 677–686.
16 Cady, W. G., *Piezoelectricity*, Vol. 1. Dover Publications Inc., Dover, NY, 1964.
17 Vinson, J. R. and Sierakowski, R. L., *The Behavior of Structures Composed of Composite Materials*. Martinus Nijhoff, Dordrecht, The Netherlands, 1987, pp. 45–49.

APPENDIX

Following are details of the finite element model development. For convenience, the mid-plane strains and curvatures [equation (20)] are presented in matrix form.

$$\varepsilon_B = \mathbf{L}_B \mathbf{u} \tag{A1}$$

where $\mathbf{L}_B$ is a derivative operator matrix defined as follows.

$$\mathbf{L}_B = \begin{bmatrix} d_x & 0 & 0 & 0 & 0 & 0 & 0 \\ 0 & 0 & d_y & 0 & 0 & 0 & 0 \\ d_y & 0 & d_x & 0 & 0 & 0 & 0 \\ 0 & d_x & 0 & 0 & -d_{xx} & -d_{xx} & -d_{xx} \\ 0 & 0 & 0 & d_y & -d_{yy} & -d_{yy} & -d_{yy} \\ 0 & d_y & 0 & d_x & -2d_{xy} & -2d_{xy} & -2d_{xy} \\ 0 & -\frac{4}{3h^2}d_x & 0 & 0 & 0 & 0 & 0 \\ 0 & 0 & 0 & -\frac{4}{3h^2}d_y & 0 & 0 & 0 \\ 0 & -\frac{4}{3h^2}d_y & 0 & -\frac{4}{3h^2}d_x & 0 & 0 & 0 \end{bmatrix} \tag{A2}$$

$$d_x = \frac{\partial}{\partial x},\ d_y = \frac{\partial}{\partial y},\ d_{xx} = \frac{\partial^2}{\partial x^2},\ d_{yy} = \frac{\partial^2}{\partial y^2} \text{ and } d_{xy} = \frac{\partial^2}{\partial x \partial y} \tag{A3}$$

and

$$\mathbf{u} = \left[u_{10}\ u_{11}\ u_{20}\ u_{21}\ u_{30}\ \frac{\partial u_{30}}{\partial x}\ \frac{\partial u_{30}}{\partial y} \right]^T \tag{A4}$$

The shear strain vector [equation (31)] is also presented in matrix form.

$$\varepsilon_T = \mathbf{L}_T \mathbf{u} \tag{A5}$$

where $\mathbf{L}_T$ is a derivative operator matrix defined as follows.

$$\mathbf{L}_T = \begin{bmatrix} 0 & 0 & 0 & 1 & 0 & 0 & 0 \\ 0 & 1 & 0 & 0 & 0 & 0 & 0 \\ 0 & 0 & 0 & -\frac{4}{h^2} & 0 & 0 & 0 \\ 0 & -\frac{4}{h^2} & 0 & 0 & 0 & 0 & 0 \end{bmatrix} \tag{A6}$$

The quantities in the statement of virtual displacements [equation (47)] are defined in terms of the force and moment resultants and mid-plane strains and curvatures as follows.

$$\begin{aligned} \delta U_B = & \int_{-h/2}^{h/2} \int_A \left(N_1 \delta\varepsilon_1^0 + N_2 \delta\varepsilon_2^0 + N_6 \delta\varepsilon_6^0\right) dA dz \\ & + \int_{-h/2}^{h/2} \int_A \left(M_1 \delta\kappa_1^0 + M_2 \delta\kappa_2^0 + M_6 \delta\kappa_6^0\right) dA dz \\ & + \int_{-h/2}^{h/2} \int_A \left(P_1 \delta\kappa_1^2 + P_2 \delta\kappa_2^2 + P_6 \delta\kappa_6^2\right) dA dz \end{aligned} \tag{A7}$$

$$\delta U_T = \int_{-h/2}^{h/2} \int_A \left(Q_2 \delta\varepsilon_5^0 + Q_1 \delta\varepsilon_4^0 + R_2 \delta\kappa_5^2 + R_1 \delta\kappa_4^2\right) dA dz \tag{A8}$$

$$\delta W = \int_A p(x,y) \delta U_3 dA dz = 0 \tag{A9}$$

Each of the five unknown functions are represented by their corresponding elemental functions $u^e(x,y)$, which are interpolated as follows.

$$u^e(x,y) = \sum_{i=1}^{N_n} N_i^e(x,y) w_i^e \tag{A10}$$

where N_n is the number of nodes,

$$N_i^e$$

are the interpolation functions and the superscript e denotes the corresponding parameter at the element level. The quantities $w_i{}^e$ are the nodal degrees of freedom defined as follows.

$$\mathbf{w}_i^e = \left[u_{10_i} \; u_{11_i} \; u_{20_i} \; u_{21_i} \; u_{30_i} \; \frac{\partial u_{30_i}}{\partial x} \; \frac{\partial u_{30_i}}{\partial y} \right]^T \tag{A11}$$

Bilinear shape functions are used for the first four unknowns, while a 12 term cubic polynomial is used for the transverse displacements (u_{30}). The resulting four noded rectangular elements are non-conforming for computational efficiency and contain 28 degrees of freedom each. The strains are represented as follows.

$$\varepsilon_B^e = \mathbf{B}_B^e \mathbf{w}^e \tag{A12}$$

$$\varepsilon_T^e = \mathbf{B}_T^e \mathbf{w}^e \tag{A13}$$

where

$$\mathbf{B}_B^e = \mathbf{L}_B \mathbf{N}^e \tag{A14}$$

$$\mathbf{B}_T^e = \mathbf{L}_T \mathbf{N}^e \tag{A15}$$

Summing over all of the elements, the finite element equations are derived using the discretized form of the principle of virtual work as follows.

$$\sum_{e=1}^{N_e} \left[\delta\mathbf{w}^e \left(\mathbf{K}^e - \mathbf{K}_P^e\right) \mathbf{w}^e - \delta\mathbf{w}^e \left(\mathbf{F}^e + \mathbf{F}_P^e\right) \right] = 0 \tag{A16}$$

where N_e is the number of elements, and

$$\mathbf{K}^e = \int_{A_e} \mathbf{B}_B^{eT} \mathbf{A}_B \mathbf{B}_B^e dA^e + \int_{A_e} \mathbf{B}_T^{eT} \mathbf{A}_T \mathbf{B}_T^e dA^e \tag{A17}$$

$$\mathbf{F}^e = \int_{A_e} \mathbf{N}_B^{eT} p^e(x,y) dA^e \tag{A18}$$

$$\mathbf{F}_P^e = \int_{A_e} \mathbf{N}_B^{eT} \mathbf{A}_a{}' \Lambda_a^e dA^e \tag{A19}$$

$$\mathbf{K}_P^e = \int_{A_e} \mathbf{B}_B^{eT} \mathbf{A}_b{}' \mathbf{B}_P^e dA^e \tag{A20}$$

The quantities $\mathbf{K}_e$ and $\mathbf{F}_e$ represent the standard stiffness matrix and force vector due to a distributed load, respectively, $\mathbf{F}_P^e$ is the force vector due to the constant portion of the piezoelectric actuation and $\mathbf{K}_P^e$ is the resultant matrix due to the strain dependent portion of the piezoelectric actuation. The matrix $\mathbf{B}_p^e$ is similar to $\mathbf{B}_B^e$ except that the elements of the first three rows corresponding to the mid-plane strains (ε_i^0, $i = 1, 2, 6$) are zero. The laminate stiffness matrices are integrated analytically through the thickness of the laminate, ply by ply, and the finite element matrices are assembled using exact or full numerical integration. It must be noted that reduced integration and shear correction factors are not needed in the current analysis. The arbitrary nature of the variation $\delta\mathbf{w}$ leads to a linear set of finite element equations [equation (48)] which are solved for the nodal displacements $\mathbf{w}$. These equations inherently determine values for the strain dependent piezoelectric coefficients in a single step without the need for iteration.